Journal of Solid State Chemistry **148,** 370–375 (1999)
Article ID jssc.1999.8462, available online at http://www.idealibrary.com on IDEAL®

Stability and Optical Properties of γ-Gd_2S_3 at High Pressures

Andrzej Grzechnik

Max-Planck-Institut für Festkörperforschung, Heisenbergstr. 1, D-70569 Stuttgart, Germany

Received April 13, 1999; accepted July 22, 1999

High pressure behavior of γ-Gd_2S_3 ($I\bar{4}3d$, $Z = 4$) is studied with X-ray diffraction, Raman spectroscopy, and optical reflectivity. Upon compression to 30 GPa there is no structural phase transition. The pressure dependence of the infrared transparency in this material to 30 GPa is determined from its bulk modulus, extracted from the X-ray data, and the pressure shift of the highest wavenumber first-order Raman mode. Optical reflectivity spectra up to 20 GPa show a red shift of the lowest energy direct interband transitions. At higher pressures, broadening of the reflectivity spectral features is associated with a loss of Raman intensity as a result of a possible transformation in the electronic structure. Free carriers do not emerge up to 35 GPa, indicating that γ-Gd_2S_3 remains semiconducting. © 1999 Academic Press

INTRODUCTION

Rare earth sesquisulfides Ln_2S_3 in the series $Ln = $ La–Dy have three polymorphs at atmospheric pressure. The α-Ln_2S_3 modifications, stable approximately to 973–1173 K, take an orthorhombic structure ($Pnma$, $Z = 4$). in which the cations are 8- and 7-fold coordinated (1). The β polymorphs, occuring between about 973 and 1373–1473 K, are in fact $Ln_{10}S_{15-x}O_x$ oxysulfides ($0 \leq x \leq 1$) with a tetragonal lattice ($I4_1/acd$, $Z = 4$) (2). The high temperature γ phases have a bcc lattice of the Th_3P_4 type ($I\bar{4}3d$, $Z = 4$), with 8-fold coordinated cations randomly distributed over available sites, $Ln_{2.67}\square_{0.33}S_4$ ($\square_{0.33}$ is the number of vacancies) (3,4). Heavier rare earth sesquisulfides ($Ln = $ Ho–Lu) have six different structural types, depending on cation radii and coordination numbers and temperature and pressure conditions (4–7). In these materials, the coordination numbers of the cations vary from six to eight and the higher coordinated polymorphs are obtained at high pressures.

Of all the known polymorphs of rare earth sesquisulfides, the γ modifications with the Th_3P_4 structure have attracted most of the attention as promising optical materials (8–12). γ-Ln_2S_3 compounds are wide-gap (2–3 eV) high-resistivity ($\sim 10^{10}\ \Omega$ cm) semiconductors (13) and far-infrared transmitting materials (14–16). Since there is no center of inversion in the Th_3P_4 structure, they satisfy the necessary condition for the existence of piezoelectric and electrooptic effects. These have been analyzed for γ-La_2S_3 and γ-Dy_2S_3 in great detail (17, 18).

Pure and doped γ-Ln_2S_3 phases are also precursor materials for several multiternary crystalline and amorphous systems (10, 11, 19, 20). Much effort has been concentrated on techniques to process these materials and to tune their optical and electronic properties (10, 11). Optical measurements on a series of Ln_2S_3 ($Ln = $ La–Lu) compounds revealed that their optical band gaps depend on the coordination numbers of the cations and on the structural types (21). High-pressure high-temperature methods of materials synthesis have already been employed to obtain different rare earth sesquisulfides, with the γ-Ln_2S_3 polymorphs among them (4–7). γ-Ln_2S_3 in the series of sesquisulfides with $Ln = $ La–Dy have the smallest volume per formula unit and the highest coordination of the cations, so that all other sesquisulfide polymorphs ($Ln = $ Ho–Lu) are expected to transform to the Th_3P_4 structure at high pressures (4). However, the question of further pressure-induced structural and electronic transformations in this group of compounds ($Ln = $ La–Lu) is still open.

In this study, the effect of pressure on the structure and optical properties of γ-Gd_2S_3 is examined using X-ray diffraction, Raman spectroscopy, and optical reflectivity measurements. This material occurs toward the end of the series of the Th_3P_4-structured rare earth sesquisulfides that can be obtained using simple synthesis methods (19, 22, 23) and does not require high pressure (4, 6) or attrition milling (24, 25) techniques of preparation. As such, it could serve as a model compound for the entire lanthanide series at high pressure conditions.

EXPERIMENTAL PROCEDURES

γ-Gd_2S_3 was obtained by heating a finely grained Gd_2O_3 powder in a silica tube furnace under a flow of H_2S. The evacuated furnace tube with the oxide in a graphite boat was purged with argon twice. The temperature was raised to 1373 K under an argon atmosphere in 8 hours. The reaction

0022-4596/99 $30.00

of the oxide with flowing H_2S proceeded at 1373 K for 8 hours. After this, the furnace was turned off and the sample was cooled down to room temperature under argon to avoid sulfur condensation. The use of the graphite boat was necessary to prevent γ-Gd_2S_3 from converting into the oxysulfide. The absence of the nonreacted starting material and α- and β-Gd_2S_3 modifications was confirmed with X-ray diffraction. The obtained γ-Gd_2S_3 product was stored in evacuated and sealed Pyrex ampules.

Energy-dispersive X-ray diffraction patterns at high pressures were recorded on the wiggler line of the DCI storage ring at the Laboratoire pour l'Utilization du Rayonnement Électromagnétique (LURE, Orsay, France). The diffracted beam was collected between 5 and 60 keV ($E \times d = 70.584 \pm 0.072$ keV × Å) using a Canberra planar germanium detector. Raman spectra were collected using a triple spectrograph (1800 groove/mm gratings) with CCD signal detection. Raman scattering was excited using an Ar^+ laser at a wavelength of 487.98 nm. Optical reflectivity spectra were recorded in the range 0.6–4 eV using a system described elsewhere (26). The sample was tightly packed in a gasket chamber to give a smooth surface in direct contact with a diamond cutlet. The spectra were corrected for absorption of the diamond and for reflection losses at its table. Pressures during all the experiments were determined from the shift of the R_1 ruby fluorescence line (27).

RESULTS AND DISCUSSION

Figure 1 shows X-ray diffraction patterns of γ-Gd_2S_3 at different pressures up to 22.1 GPa. Peak indices for all the patterns are consistent with $I\bar{4}3d$ symmetry, indicating that there is no phase transition. The third-order Birch–Murnaghan equation of state (28) was used for fitting the pressure dependence of the unit cell volume (Fig. 2). The extracted unit cell volume at zero pressure (V_0), isothermal bulk modulus (K_0), and its first pressure derivative (K'_0), both at zero pressure, are 588.52 (0.78) Å^3, 101.0 (2.8) GPa, and 1.6 (0.2), respectively. The K'_0 parameter determines the curvature in the pressure dependence of the unit cell volume. Its value for three dimensional structures, as determined by the third order Birch–Murnaghan equation for state, is

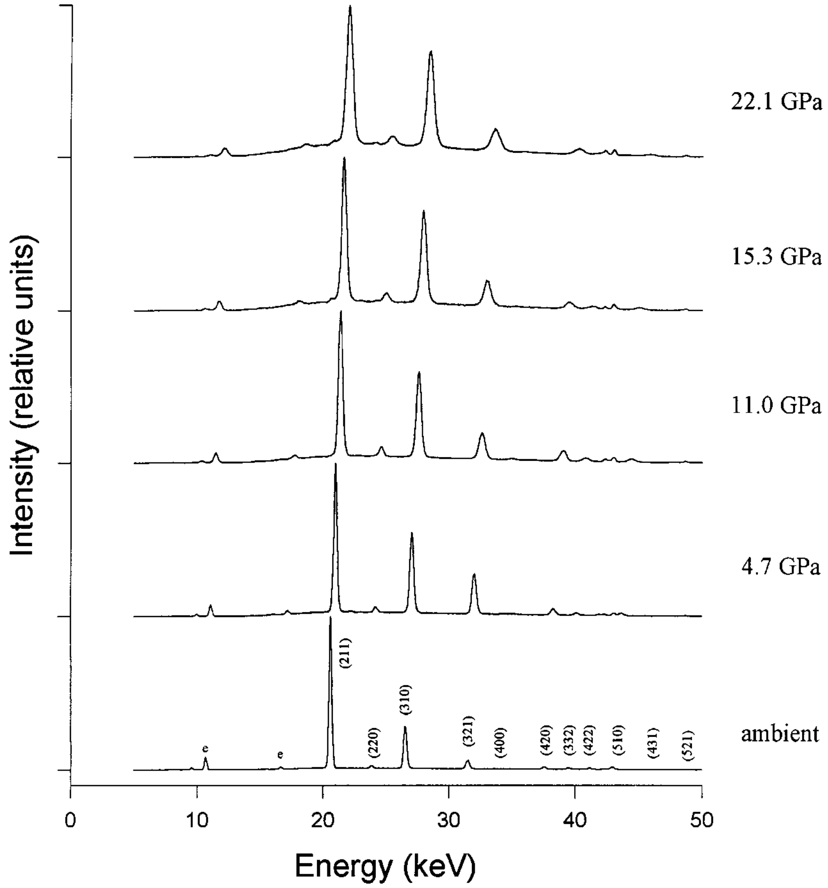

FIG. 1. Energy-dispersive X-ray diffraction patterns of γ-Gd_2S_3 at high pressures. Symbols in brackets are Miller indices. The symbol, "e" indicates escape peaks. All patterns are vertically offset for clarity.

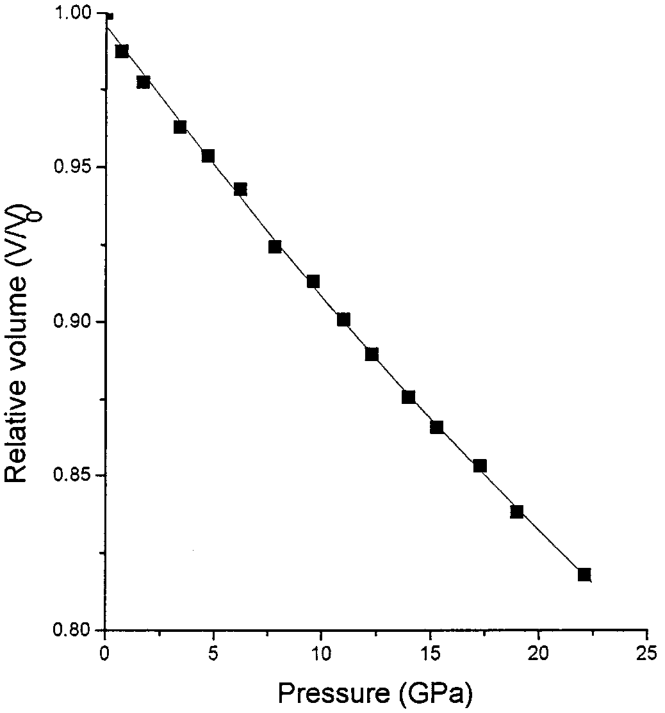

FIG. 2. Relative volume of the γ-Gd$_2$S$_3$ unit cell as a function of pressure.

usually very close to 4.0. The low value of $K'_0 = 1.6$ for γ-Gd$_2$S$_3$ can be attributed to the presence of defects and vacancies in the structure so that the bulk compression is partly taken up by local compression around empty sites in the crystal lattice.

Raman spectra of γ-Gd$_2$S$_3$ at high pressures are presented in Fig. 3. The spectrum at ambient conditions closely corresponds to the ones of other γ polymorphs, reported by Arkatova *et al.* (15) and Knight and White (16). Optical modes in the Th$_3$P$_4$ type (T^6d) are distributed as A_1 (Raman) + $2A_2$ (inactive) + $3E$ (Raman) + $5T_1$ (inactive) + $5T_2$ (Raman + infrared) (29). Since there is no center of inversion in this structure, the triply degenerate T_2 modes are both Raman and infrared active. The A_1 mode involves only oscillations of the sulfur atoms. According to Arkatova *et al.* (15), the Raman bands above 200 cm^{-1} agree with infrared absorption bands, so they should be attributed to the strong polar T_2 modes. On the other hand, Knight and White (16) assigned the Raman band at about 250 cm^{-1} to the A_1 mode. They argued that its anomalous broadening is due to the presence of vacancies ($\square$) on both cation and anion sublattices, $Ln_2\square S_3\square$.

Upon compression, all the Raman bands in γ-Gd$_2$S$_3$ shift monotonously toward higher wavenumbers (Fig. 4). At pressures above about 20 GPa, there occurs a gradual change in intensity of the scattered Raman signal from the sample (Fig. 3). However, it is not associated with any additional anomaly in the pressure shift of the observed bands, that would suggest a structural phase transition. Upon decompression, all the intensity changes in the spectra are reversible.

As discussed earlier, the highest wavenumber Raman band corresponds to the T_2 mode that is also infrared allowed. Its wavenumber determines the position of the phonon edge and, as a consequence, the long wavelength limit of infrared transparency in this material. This limit is a basic parameter for evaluation of compounds for long wavelength transmitting devices (8). The phonon edge energy covers a multiphonon region of the vibrational modes and is determined at twice the highest wavenumber fundamental phonon (30). The phonon edge for γ-Gd$_2$S$_3$ occurs at about 600–620 cm^{-1} (16.66–16.13 μm). From the evolution of the Raman band at about 310 cm^{-1}, it can be inferred that the pressure dependence of the phonon edge, $\partial v/\partial P$, is equal to 7.2 (0.4) cm^{-1}/GPa. The pressure dependence of the far-infrared phonon edge can be correlated with the pressure dependence of the unit cell volume through a microscopic Grüneisen parameter (γ) at constant temperature $T = 298$ K, $\gamma = (\partial \ln v/\partial \ln V) = (K_0/v_0)(\partial v/\partial P)$, where

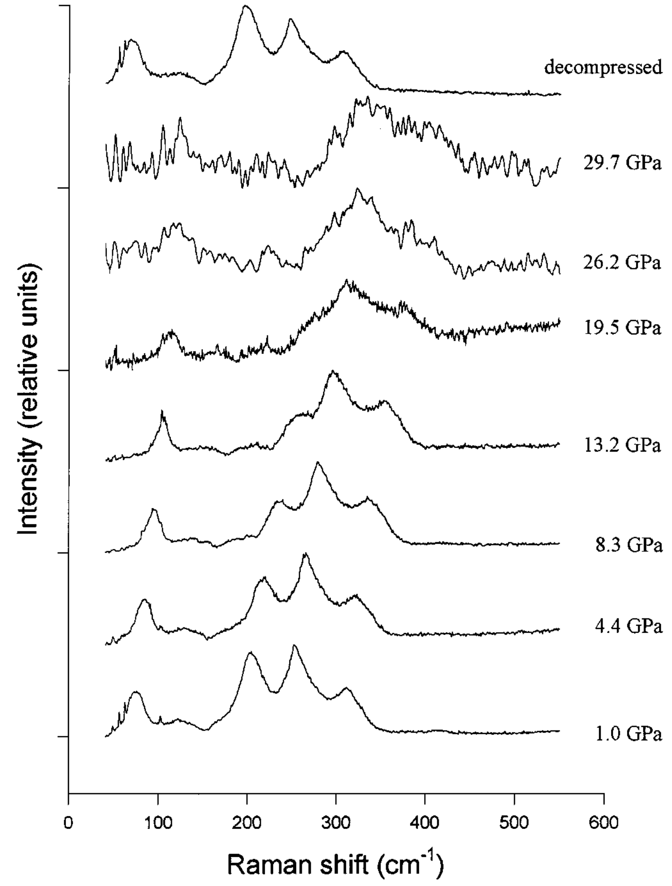

FIG. 3. Raman spectra of γ-Gd$_2$S$_3$ at high pressures. All spectra are vertically offset for clarity.

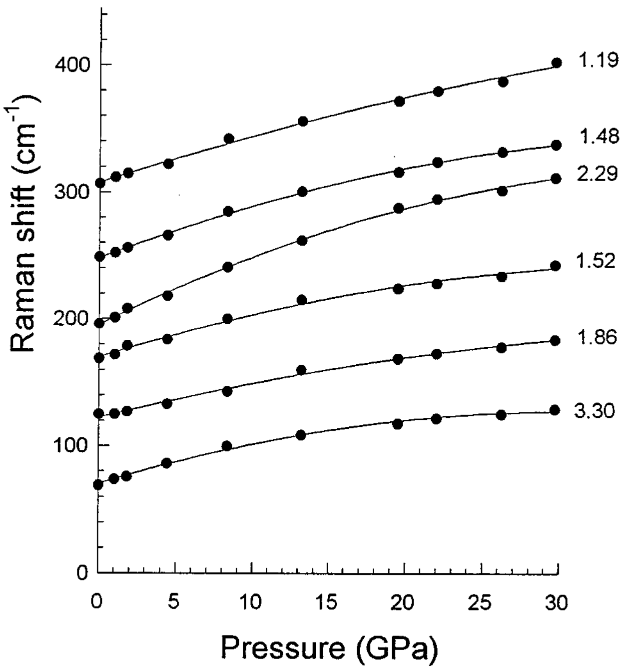

FIG. 4. Pressure dependence of Raman bands. The numbers stand for Grüneisen parameters of the observed bands.

ν is the wavenumber of the phonon edge (cm^{-1}), V is the corresponding unit cell volume (Å^3), P is the corresponding pressure, K_0 is the bulk modulus extracted from the X-ray data (GPa), and ν_0 is the position of the edge at ambient conditions (cm^{-1}). The resulting γ parameter is 2.3. Grüneisen parameters for all the vibrational modes are given in Fig. 4.

The fundamental optical band gaps in the γ-Ln_2S_3 compounds originate from the separation between the $3p$(S) valence band at the M point and the $5d$(Ln) conduction band at the Γ point of the Brillouin zone (13, 31). The energy dependence of the ε_2 imaginary part of the ε dielectric function ($\varepsilon = \varepsilon_1 + i\varepsilon_2$) provides information on direct interband transitions at higher energies than the indirect fundamental absorption band (13, 31). Witz *et al.* (32) deduced that in γ-Gd_2S_3 the values of the indirect gap and of the lowest direct interband transition are equal to 2.75 and 3.4 eV, respectively.

The measurements of the fundamental absorption band of powdered γ-Gd_2S_3 at all pressures were not feasible in this study because the sample was not transparent in a diamond anvil cell, regardless of the actual sample thickness. Similar problems have already been encountered in optical absorption measurements at ambient pressure, outside of the diamond cell (32). Such effects could be of a general nature as the structure of γ-Gd_2S_3 is intrinsically disordered, with vacancies at the cation, and possibly anion (16), sites. This could result in the low energy "tail" of the absorption edge, making the sample poorly transparent in the visible and near-infrared regions. At present, it is not clear whether the degree of disordering at the cation and anion sites depends on how the powder and single crystal samples are prepared (10, 22, 23, 32).

Figure 5 shows optical reflectivity spectra of γ-Gd_2S_3 at pressures up to 35.0 GPa. The low overall reflectivity at all pressures is due to a small difference in the refractive indices of the sample and the diamond window. The red shift of the high energy reflectivity edge indicates that the lowest energy direct interband transitions of γ-Gd_2S_3 shift toward lower energies. There is no evidence for the increase of reflectivity in the low energy infrared region due to an emergence of free carriers that would signal a transition (or a tendency toward it) into a metallic state. The reflectance spectra suggest that the oscillator strength just above the band gap due to the direct interband transitions (13, 32) does not change significantly with increasing pressure up to 20 GPa. At higher pressures, the optical edge broadens and the reflectivity at high energies decreases (the inset in Fig. 5). According to the Raman data, these changes in optical reflectivity are not due to any structural phase transition. On the other hand, they may be related to a loss of Raman intensity at pressures above 20 GPa.

At atmospheric pressure, the γ-Ln_2S_3 compounds, with vacancies randomly distributed in the crystal lattice, are wide-gap high-resistivity semiconductors (13, 21). Corresponding mixed valence Ln_3S_4 materials, with the same structure, are metallic (33). As the optical reflectivity at the near infrared limit shows, free carriers do not emerge with increasing pressure up to 35.0 GPa, indicating that γ-Gd_2S_3 does not transform (or does not tend to transform) into a metallic. From a lack of significant reflectivity changes at the high energy limit (about 4 eV) at pressures up to 20 GPa, one could infer that the scheme of the direct interband transitions (13, 32) is preserved with closure of the band gap. Raman intensity and optical reflectivity data collected at higher pressures indicate a possible change in the electronic structure of this material, associated with different direct interband transitions. There is no corresponding anomaly in the pressure dependence of the phonon edge, i.e., the infrared transparency of γ-Gd_2S_3. The present data do not allow us to draw any conclusions about a possible pressure-induced ordering of vacancies at the cationic and anionic sites in the crystal lattice and the electronic structure.

The data of this study indicate that γ-Gd_2S_3 does not undergo any structural phase transition up to 30 GPa. One of the mechanisms for a possible structural change is an increase of coordination around the gadolinium atoms. This would be a driving force to achieve a higher density phase. γ-Ln_2S_3 compounds have the smallest volume per formula unit and the highest 8-fold coordination of the cations in the rare earth sesquisulfide group at ambient conditions, so that all other polymorphs are expected to transform to the

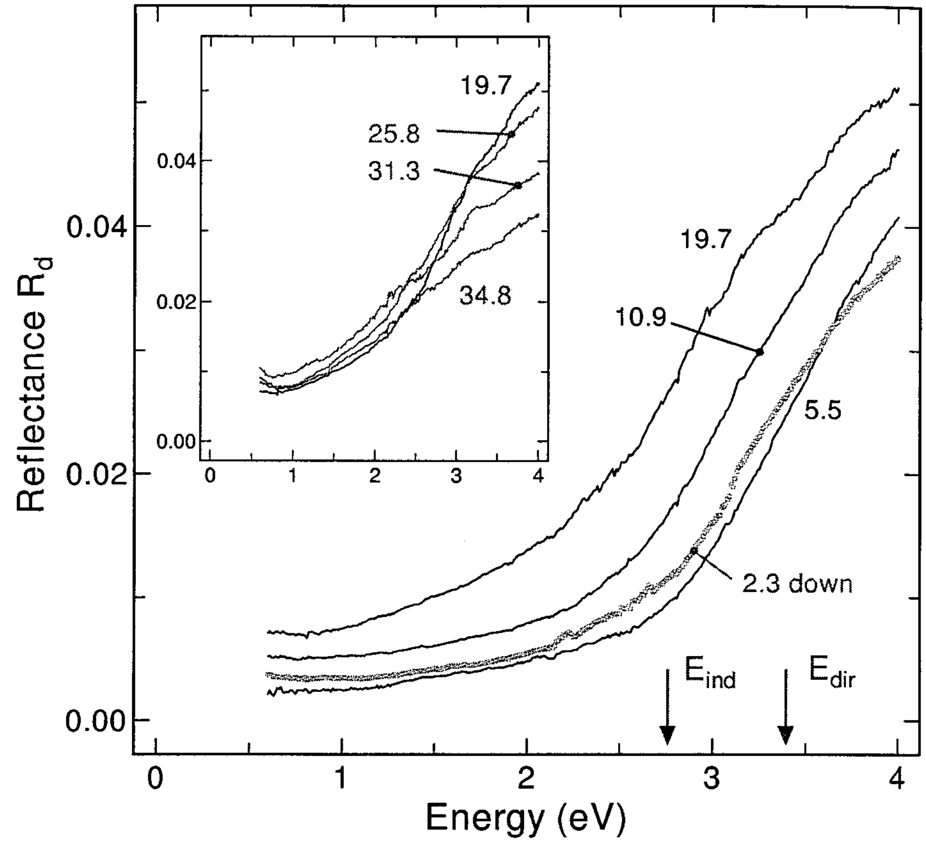

FIG. 5. Optical reflectivity spectra of γ-Gd_2S_3 at high pressures. The reflectivity R_d is measured at the diamond–sample interface. The positions of edges corresponding to the indirect (E_{ind}) and direct (E_{dir}) transitions at ambient pressure (32) are marked with arrows. The numbers stand for pressures in GPa. There is no vertical offset of the spectra.

Th_3P_4 structure at high pressures (4). The stability of γ-Gd_2S_3 at high pressures suggests that the 8-fold cation coordination is the maximum one for this stoichiometry, unlike the 9-fold one in stochiometric and nonstochiometric lanthanide disulfides (34, 35). One would expect that a quenchable pressure-induced phase transition in γ-Ln_2S_3, associated with an increase of a cationic coordination, would not probably yield materials with lower phonon edges, i.e., with better transmitting properties in infrared.

In chemically and structurally related alkaline earth–rare earth sulfides and cadmium sulfide–rare earth sulfides, the Th_3P_4 type occurs along with the $MgAl_2O_4$ spinel (*Fd*3*m*) and $CaFe_2O_4$ (*Pnma*) structures (21). At atmospheric conditions $MgTm_2S_4$ and $MgYb_2S_4$ have a structure of spinel and by pressurizing them at 5.5 GPa and 1473 K, the phases of the Th_3P_4 type, with the Mg^{2+} and lanthanide cations randomly distributed at the available sites, can be recovered (36). It shows that various structural types of chalcogenide materials—e.g., spinel and calcium ferrite (36), corundum and bixbyite (4)—converge into the noncentrosymmetric structure of thorium phosphide, further stable at high pressures. For some oxide compounds, the pressure-induced structural changes proceed along the path spinel → calcium ferrite (37); however, the Th_3P_4-type phases have not been observed yet. The best candidates for high pressure Th_3P_4-structured oxides would be the analogues of alkaline earth–rare earth sulfides of the $CaFe_2O_4$ type, e.g., $MeLn_2O_4$ (Me = Ca, Sr, Ba; Ln = La–Lu). In addition, the cubic bixbyite structure (*Ia*3) of Yb_2S_3 and Tm_2S_3 (6), with 6-fold coordinated cations, is a common one for the rare earth oxides (the C-type (38). It is not yet known whether the C-type lanthanide oxides would transform into the Th_3P_4 structure at high pressures and temperatures.

ACKNOWLEDGMENTS

I thank Alain Lafond and Ulrich Oelke for their assistance with sample preparations and optical reflectivity measurements, respectively. I carried out the X-ray measurements during my post-doctoral stay at the Laboratoire de Physico-Chimie des Materiaux Luminescents, Universite Claude Bernard Lyon I (France).

REFERENCES

1. C. T. Prewitt and A. W. Sleight, *Inorg. Chem.* **7,** 1090 (1968).
2. T. Schleid and F. Lissner, *J. Less-Common Met.* **175,** 309 (1991).
3. W. H. Zachariasen, *Acta Cryst.* **2,** 57 (1949).
4. K.-J. Range, K. G. Lange, and H. Drexler, *Comm. Inorg. Chem.* **3,** 171 (1984).
5. K.-J. Range, A. Gietl, U. Klement, and K. G. Lange, *J. Less-Common Met.* **158,** L21 (1990).
6. T. Schleid and F. Lissner, *Z. Natur.* **51b,** 733 (1996).
7. K.-J. Range, A. Gietl, and M. Andratschke, *Z. Krist.* **212,** 138 (1997).
8. P. N. Kumta and S. H. Risbud, *J. Mater. Sci.* **29,** 1135 (1994).
9. V. V. Sokolov, A. A. Kamarzin, L. N. Trushnikova, and M. V. Savelyeva, *J. Alloys Comp.* **225,** 567 (1995).
10. T. M. Batirov, V. M. Fridkin, and A. A. Kamarzin, *Phys. Status Solidi A* **65,** K163 (1984).
11. A. N. Georgobiani, V. I. Demin, and E. S. Logozinskaya, *Tr. Fiz. Inst. Akad. Nauk SSSR* **182,** 69 (1987).
12. R. Mauricot, J. Bullot, J. Wery, and M. Evain, *Mater. Res. Bull.* **31,** 263 (1996).
13. V. P. Zhuze and A. I. Shelykh, *Fiz. Tekh. Poluprovodn.* **23,** 393 (1989).
14. G. N. Kustova, K. F. Obzherina, A. A. Kamarzin, E. V. Dulepov, S. S. Derbeneva, and S. S. Batsanov, *Zhur. Struct. Khimii* **10,** 609 (1969).
15. T. G. Arkatova, V. P. Zhuze, M. G. Karin, A. A. Kamarzin, A. A. Kukharskii, B. A. Mikhailov, and A. I. Shelykh, *Fiz. Tverd. Tela* **21,** 3428 (1979).
16. D. S. Knight and W. B. White, *Spectrochim. Acta A* **46,** 381 (1990).
17. T. I. Volkonskaya, A. I. Shelykh, V. V. Sokolov, and I. A. Smirnov, *Fiz. Tverd. Tela* **27,** 684 (1985).
18. T. I. Volkonskaya, A. I. Shelykh, A. V. Sotnikov, V. V. Sokolov, and F. R. Akhmetdzhanov, *Fiz. Tverd. Tela* **29,** 559 (1987).
19. C. M. Vaughan-Forster and W. B. White, *J. Amer. Ceram. Soc.* **80,** 273 (1997).
20. M. M. Asadov and M. M. Abbasov, *Neorg. Mater.* **32,** 313 (1996).
21. O. Schewciw and W. B. White, *Mater. Res. Bull.* **18,** 1059 (1983).
22. S. Roméro, A. Mosset, J.-C. Trombe, and P. Macaudière, *J. Mater. Chem.* **7,** 1541 (1997).
23. F. Marrot, A. Mosset, J.-C. Trombe, P. Macaudière, and P. Maestro, *J. Alloys Comp.* **259,** 145 (1997).
24. S. H. Han, K. A. Gschneidner, Jr., and B. J. Beaudry, *Scripta Metall. Mater.* **25,** 295 (1991).
25. S. H. Han, K. A. Gschneidner, Jr., and B. J. Beaudry, *J. Alloys Comp.* **181,** 463 (1992).
26. K. Syassen and R. Sonnenschein, *Rev. Sci. Instrum.* **53,** 644 (1982).
27. H. K. Mao, P. M. Bell, J. W. Shaner, and D. J. Steinberg, *J. Appl. Phys.* **49,** 3276 (1978).
28. F. Birch, *J. Geophys. Res.* **83,** 1257 (1978).
29. S. Bhagavantam and T. Venkatarayudu, "Theory of Groups and its Applications to Physical Problems," 2nd ed. Andhra University Press, Waltair, 1951.
30. W. B. White, *Proc. SPIE* **1326,** 80 (1990).
31. V. Zhukov, R. Mauricot, P. Gressier, and M. Evain, *J. Solid State Chem.* **128,** 197 (1997).
32. C. Witz, D. Huguenin, J. Lafait, S. Dupont, and M. L. Theye, *J. Appl. Phys.* **79,** 2038 (1996).
33. H. Bergmann, *in* "Gmelin Handbook of Inorganic Chemistry," C7, 8th ed. Springer-Verlag, Berlin, 1983.
34. J. Flahaut, *in* "Handbook on the Physics and Chemistry of Rare Earths" (K. A. Gschneider, Jr., and L. Eyring, (Eds.), Vol. 2, North-Holland, Amsterdam, 1979.
35. A. Grzechnik, *Physica B* **262,** 426 (1999).
36. K. Hirota, N. Kinomura, S. Kume, and Koizumi, *Mater. Res. Bull.* **11,** 227 (1976).
37. H. Yamada, Y. Matsui, and E. Ito, *Mineral. Mag.* **47,** 177 (1983).
38. E. N. Maslen, V. A. Streltsov, and N. Ishizawa, *Acta Cryst. B* **52,** 414 (1996).